Self-assembly of two-dimensional nanoclusters observed with STM: From surface molecules to surface superstructure

Canhua Liu,* Iwao Matsuda, Marie D'angelo, and Shuji Hasegawa
Department of Physics, School of Science, University of Tokyo, 7-3-1 Hongo, Bunkyo-ku, Tokyo 113-0033, Japan

Jun Okabayashi, Satoshi Toyoda, and Masaharu Oshima
Department of Chemistry, School of Engineering, University of Tokyo, 7-3-1 Hongo, Bunkyo-ku, Tokyo 113-0033, Japan
(Received 2 May 2006; revised manuscript received 4 September 2006; published 13 December 2006)

A type of stable and identical two dimensional (2D) Au nanoclusters are discovered to exist on the Si(111)-$\sqrt{3}\times\sqrt{3}$-Ag surface at submonolayer Au coverage. Self-assembly of these Au nanoclusters leads to a 2D superstructure Si(111)-$\sqrt{21}\times\sqrt{21}$-(Ag+Au). This discovery helps us to obtain definite evidence that all the previously proposed atomic structure models for the $\sqrt{21}\times\sqrt{21}$ structure can be excluded. A model in which three Au adatoms locate on Ag triangles in the $\sqrt{21}\times\sqrt{21}$ unit cell is built based on the low-temperature scanning tunneling microscopy observations. Additionally, the stability and the uniformity of the Au nanocluster are discussed in terms of a substrate-mediated interaction among the Au adatoms, and the self-assembling process is understood by analogizing the Au nanocluster with a kind of surface molecule.

DOI: 10.1103/PhysRevB.74.235420 PACS number(s): 68.43.Fg, 68.43.Hn, 68.37.Ef, 68.47.Fg

I. INTRODUCTION

Metal nanoclusters have become a target of intensive research because of interests from their fundamental physics, catalysis, and potential applications to devices.[1,2] Fabrication of uniform-size cluster arrays at the ultrasmall 1–2 nm size regime is highly desirable for exploring novel physical phenomena and practical device applications. Self-assembly of nanoclusters on a crystal surface due to so-called template effect is one of the promising approach to the purpose, and it has been turned out that a Si(111)-7×7 surface is an ideal template due to its dangling bonds which may assign periodic adsorption sites to foreign atoms.[3–5] Li, Jia, and their collaborators showed recently that periodic arrays of identical metal nanoclusters can be fabricated on the Si(111)-7×7 surface by delicate control of growth kinetics during adsorptions of metal atoms, e.g., In, Ag, Mn, Al, and Ga.[6,7] These nanocluster arrays follow exactly the substrate periodicity and exhibit remarkable stability due to strong chemical bonding between adsorbate atoms and substrate atoms. Thus, the role of interactions among nanoclusters is negligible in this kind of self-assembly process.

On a smooth surface where adsorbates bond to the substrate weakly, on the contrary, the interactions among adatoms should have more important influence on the formation of nanostructures. On metal surfaces, for example, surface-state mediated adatom interactions are believed to play significant roles in atomic self-assembly.[8] Such a substrate-mediated interaction has been well described by asymptotic theories if the separation between adatoms is sufficiently large, i.e., the interaction decays with adsorbate separation d as d^{-2} and oscillates with a period related to the Fermi wave vector of surface-state electrons.[9,10] At "intermediate" separations where they are too long for formation of direct chemical bonds and too short for the asymptotic regime, density-functional theory (DFT) calculations show that these interactions can be strong enough to influence the sizes and shapes of nanostructures on surfaces.[11] Thus, it is speculated that metal adatoms can gather to form nanoclusters and self-assemble into periodic arrays on a smooth surface even if the adsorbate-substrate interacitons are very weak. This should be contrasted to the self-assembling due to the template effect of substrate as on the Si(111)-7×7 surface.[3–7]

In another point of view, periodically arranged identical nanoclusters actually form a type of surface superstructures whose building blocks are recognizable. In other words, a superstructure constructed from stable and identical nanoclusters on a smooth surface may give an affirmative evidence to the above speculation.

A monolayer-Ag-terminated Si(111) surface, the Si(111)-$\sqrt{3}\times\sqrt{3}$-Ag surface ($\sqrt{3}$-Ag in short hereafter), may be an ideal substrate for studying this issue because of its intactness against adsorbates. This is due to no dangling bonds remaining on the $\sqrt{3}$-Ag surface, in contrast to the 7×7 clean surface. In addition, it has a surface state of two-dimentional nearly-free electron gas (2DEG) which can mediate the indirect electronic adatom-adatom interactions. A wide variety of metal atoms[12] and molecules[13–15] have been deposited on the $\sqrt{3}$-Ag surface for exploring new nanostructures and physical phenomena. An interesting thing is that adsorptions of monovalent atoms including noble and alkali metals onto the $\sqrt{3}$-Ag surface commonly induce $\sqrt{21}\times\sqrt{21}$ surface superstructures that have elevated surface electrical conductivities comparing to the $\sqrt{3}$-Ag substrate.[12,16] Photoelectron spectroscopy (PES) studies have revealed the surface-state bands of the $\sqrt{21}\times\sqrt{21}$ superstructures and succeeded in explaining their elevated electrical conductivity.[17–23] But their atomic structures are still under debate and the formation mechanism is unclear, in spite of many studies of scanning tunneling microscopy (STM),[17,24–27] surface x-ray diffraction (SXRD),[28] and reflection-high-energy positron diffraction (RHEPD).[29]

In this report, we study the formation mechanism of the Si(111)-$\sqrt{21}\times\sqrt{21}$-(Ag+Au) superstructure ($\sqrt{21}$-Au in short hereafter, which is formed by depositing submonolayer Au on the $\sqrt{3}$-Ag) by using the concepts of self-assembly of

nanoclusters and substrate mediated interatomic interactions. Different from the previous STM studies that had been performed only on the $\sqrt{21}$-Au superstructure itself at room temperature (RT),[24,25] we investigate its formation process by changing the Au coverages and performing STM at low temperature (LT) (~65 K). We have observed stable and identical Au nanoclusters at very low Au coverages, and they aggregate into the $\sqrt{21}$-Au superstructure as the Au coverage increases. A serious analysis is performed on the obtained STM images, which could not be explained by any of the previously proposed atomic structure models of the $\sqrt{21}$-Au surface. Based on the STM observations, therefore, we proposed a model in which three Au adatoms locate on the Ag triangles in the $\sqrt{21}\times\sqrt{21}$ unit cell. This new model is consistent with the Si $2p$ core-level(CL) photoemission spectroscopy (PES). Additionally, we speculate that it might be the surface-state mediated interaction among the Au adatoms that plays crucial roles in the stability and self-assembly of the Au nanoclusters. By analogizing the Au nanocluster with a surface molecule that has characteristic localized electronic states, "molecular orbits," we conceptually depict the self-assembling process as a result of nucleation of surface molecules. In other words, this surface superstructure can be regarded as a kind of supramolecular structure.

II. EXPERIMENT

Experiments were performed in two separate UHV chambers for STM and PES experiments, respectively. The LT-STM (UNISOKU-USM 501) chamber is in our laboratory, equipped with a reflection-high-energy electron diffraction (RHEED) system, and the PES chamber is on the beam line of BL-1C at the Photon Factory in KEK, Tsukuba, Japan, equipped with a low-energy electron diffraction (LEED) system and an electron analyzer of Scienta-100 with an energy resolution of ~20 meV used. The base pressure in both UHV chambers was better than 5×10^{-11} Torr. For the STM experiment, we used electrochemically sharpened W tips which were cleaned *in situ*, and all STM images were obtained in a constant-current mode.

A B-doped p-type Si(111) wafer with resistivity of 1–10 Ω cm at RT was used. After outgassing at ~400 °C overnight, the wafer was flashed at 1250 °C several times by direct current heating to obtain a clean Si(111)-7×7 surface. The $\sqrt{3}$-Ag surface was prepared at a substrate temperature of 450 °C by depositing about one monolayer [ML, 1 ML equals 7.8×10^{14} cm^{-2}, density of the most top Si atoms in the ideal Si(111)-1×1 surface] of Ag atoms. About two minutes' post-annealing at the same temperature was proceeded to remove excess Ag atoms on the $\sqrt{3}$-Ag surface. After various amounts of Au atoms were deposited on the $\sqrt{3}$-Ag surface at RT, the sample was transferred to a cold stage kept at about 65 K(70 K) for the STM (PES) experiment.

In the STM and PES experiments, the Au evaporators were roughly calibrated separately with RHEED and LEED, respectively, by making a sequence of Au/Si(111) phases at optimal coverages:[30,31] 5×2 (0.44 ML), $\alpha-\sqrt{3}\times\sqrt{3}$ (2/3 ML) and $\beta-\sqrt{3}\times\sqrt{3}$ phases (1 ML). More precise Au coverage in STM image was estimated by combining with the STM images of the Au adsorbed $\sqrt{3}$-Ag surface. Details about this coverage estimation will be mentioned in the next section. In the PES experiment, the precise Au coverage was estimated by measuring the Au $4f$ CL-PES, taking the 5×2 phase as a reference since it exhibits a complete 5×2 LEED pattern only in a very narrow Au coverage range around 0.44 ML.[30]

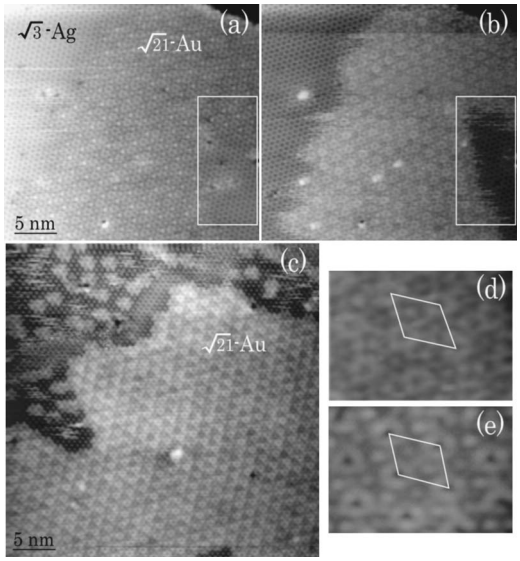

FIG. 1. Topographic STM images of the $\sqrt{21}$-Au superstructure taken at RT successively on a same area (a) V_{tip}=1.50 V, I=0.50 nA, (b) V_{tip}=−1.00 V, I=0.50 nA, and at 65 K, (c) V_{tip}=−1.50 V, I=0.60 nA. (d) and (e) are enlarged STM images taken at RT and 65 K, respectively, with a same tip bias V_{tip}=−1.00 V.

III. RESULTS AND DISCUSSION

A. Self-assembly of Au nanoclusters

All of the previous STM studies on the $\sqrt{21}$-Au superstructures were performed only at RT.[24,25] A remarkable feature is noticed in the RT-STM images shown in Figs. 1(a) and 1(b) that the $\sqrt{21}$-Au domain boundary changes successively and appears vague. This indicates incessant attachment and detachment of Au atoms at the periphery of $\sqrt{21}$-Au domain and the existence of migrating Au adatoms on the domains of $\sqrt{3}$-Ag substrate. Since the Au adatoms may migrate with a high mobility [2D adatom gas (2DAG) state], we cannot image them directly so that nothing is observed on the $\sqrt{3}$-Ag domain [upper left in Fig. 1(b)]. This proposal is proved by the LT-STM image taken at 65 K shown in Fig. 1(c). It is seen that there are many nanoclusters distributing on the $\sqrt{3}$-Ag domain [upper left in Fig. 1(c)], which can never be observed at RT. It is easy to understand that the Au adatoms in 2DAG phase at RT have lost their mobility by cooling and nucleate into nanoclusters on the $\sqrt{3}$-Ag domain, so that the domain boundary of $\sqrt{21}$-Au do not change any more. However, the temperature lowering does not induce any change in the superstructure of $\sqrt{21}$-Au itself; the STM

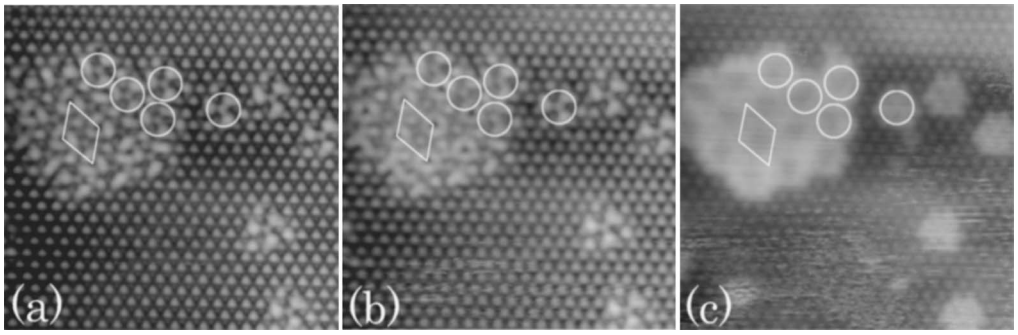

FIG. 2. Topographical STM images of an identical area of the Au-adsorbed $\sqrt{3}$-Ag surface taken at different bias voltages: (a) $V_{tip}=-0.30$ V, (b) $V_{tip}=-1.00$ V, (c) $V_{tip}=-1.80$ V. The same tunneling current of $I=0.75$ nA was set. The size of each image is 15.4×14.9 nm^2.

image taken at low temperature is almost identical with that at RT for the same bias voltage, as shown in Figs. 1(d) and 1(e). This allows to directly compare our LT-STM images with the RT-STM results previously reported.

Such a 2DAG phase has been also reported in the addtional Ag adsorptions on the $\sqrt{3}$-Ag surface. Previous LT-STM observations[32,33] revealed that the Ag 2DAG at RT aggregates to form nanoclusters that distribute randomly on the $\sqrt{3}$-Ag surface at 6 K and exhibit similar STM images as those of Au nanoclusters in Figs. 1(c) and 2. When the additional Ag atoms are deposited onto the $\sqrt{3}$-Ag surface at LT, a superstructure of Si(111)-$\sqrt{21}\times\sqrt{21}$-(Ag+Ag) ($\sqrt{21}$-Ag in short hereafter) is formed, and it exhibits very similar STM images as those of $\sqrt{21}$-Au in Figs. 1(d) and 1(e).

By depositing a small amount of Au on the $\sqrt{3}$-Ag substrate at RT and cooling it down to 65 K, we obtained a small domain of the $\sqrt{21}$-Au superstructure together with isolated identical Au nanoclusters in the same frame of STM image as shown in Fig. 2. The $\sqrt{21}\times\sqrt{21}$ unit cell is indicated with a white quadrilateral. Both the Au nanoclusters and $\sqrt{21}$-Au superstructure exhibit the same bias dependence in the STM images, which indicates a close relation between them. Giving a sign of an Au nanocluster with a circle, we find that the $\sqrt{21}$-Au domain can be divided into Au nanoclusters with the same circles (see Fig. 2). In other words, the superstructure of $\sqrt{21}$-Au can be viewed as a periodic arrangement of the identical Au nanoclusters. Actually, all the $\sqrt{21}$-Au domain can be exactly covered by such circles at any bias voltages. Furthermore, the $\sqrt{21}$-Au unit cell consists of one Au nanocluster only, which means that the Au nanoclusters can be regarded as the basic building block of $\sqrt{21}$-Au superstructure.

This finding confirms our conjecture that the superstructure of $\sqrt{21}$-Au is a self-assembly of the Au nanoclusters. It is further verified by a series of STM images at various Au coverages as shown in Fig. 3. At very low Au coverage [0.016 ML in Fig. 3(a)], only identical Au nanoclusters are observed to distribute randomly on the $\sqrt{3}$-Ag substrate. It is widely accepted now that the $\sqrt{3}$-Ag surface at LT has an atomic structure of a so-called inequivalent-triangle (IET) model,[34] which displays a hexagonal-lattice pattern in the STM images; one of the half-unit-cell Ag triangles is brighter than the other half. Because of the asymmetry of the IET structure, two types of $\sqrt{3}$-Ag domains in twin relation to each other are created, with a surface twin boundary (TB) between them. Sato *et al.* named these two domains IET− and IET+.[35] In Fig. 3(a), several TB's are observed to separate the $\sqrt{3}$-Ag substrate into IET− and IET+ domains. It is noticed that the Au nanoclusters on these different twin domains appear to rotate a little with each other. In Fig. 3(a), two triangles separated by a TB are drawn on two Au nanoclusters for the eyes' guide.

When the Au coverage is increased up to 0.048 ML as shown in Fig. 3(b), several small domains of the $\sqrt{21}$-Au superstructure are formed. Two quadrilaterals have been drawn to show the $\sqrt{21}$-Au unit cells on different domains of IET+ and IET−. They rotate by ±10.89° with respect to $[11\bar{2}]$ Si crystal orientation, respectively. It is worth noting that the two domains of $\sqrt{21}$-Au are formed on different twin domains of the $\sqrt{3}$-Ag substrate, one on the IET− and the other on the IET+ domain. This indicates that the formation of the double domains of $\sqrt{21}\times\sqrt{21}$ is due to the double domains in twin relation of the $\sqrt{3}$-Ag substrate. It should be noted here that the Au adatoms were deposited at RT and the double-domain $\sqrt{21}$-Au structure was formed at RT (though the present STM observations were done at LT). This means that the IET structure exist basically even at RT. This fact may shed a light on the debate about the RT-structure of the $\sqrt{3}$-Ag surface.[36–40]

If the Au coverage reaches a saturation value of 0.143 ML (this value will be explained later, as well as the way to estimate the Au coverages), the surface is covered completely by the $\sqrt{21}$-Au superstructure. Figure 3(c) shows an STM image taken at Au coverage of 0.136 ML, in which a large single $\sqrt{21}$-Au domain is observed.

Depositing Au atoms at RT, as we did for the above STM observations, is important for the self-assembling process. When they were evaporated at a low temperature (~135 K) onto the $\sqrt{3}$-Ag surface, however, we found by RHEED observation that the $\sqrt{21}$-Au phase was not formed. It is not difficult to understand since the Au atoms may lose their migration mobility before aggregating into clusters or the $\sqrt{21}$-Au superstructure.

The series of LT-STM images at various Au coverages in Fig. 3 thus demonstrate clearly the process of self-assembly of the Au nanoclusters into the $\sqrt{21}$-Au superstructure. It is interesting to note that no single Au atoms or other types of

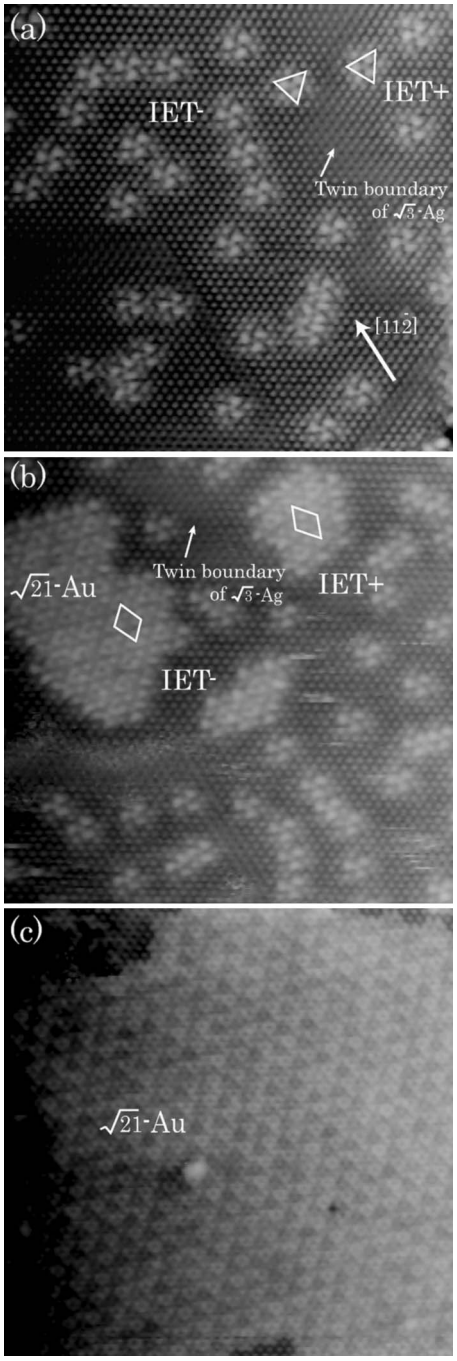

FIG. 3. Topographic STM images of Au-adsorbed $\sqrt{3}$-Ag surface at various Au coverages: (a) 0.016 ML, $V_{tip}=-0.50$ V, $I=0.75$ nA, (b) 0.048 ML, $V_{tip}=-0.50$ V, $I=0.75$ nA, (c) 0.136 ML, $V_{tip}=-1.50$ V, $I=0.50$ nA. The size of each image is 31.2×31.2 nm^2.

Au clusters have been observed in the LT-STM images. Actually this is a strong evidence for us to think that the most stable form for the low-coverage Au atoms on the $\sqrt{3}$-Ag surface is the dispersed Au nanoclusters: there were no smaller clusters. When the Au coverage is increased, the Au clusters have to aggregate into the $\sqrt{21}$-Au superstructure because there may be no enough space for them to disperse. Since all Au nanoclusters have an identical atomic structure and form the superstructure as building block, we analogize them with surface molecules that are assembled to build supramolecular nanostructures by intermolecular bonding interactions.[41] Such a point of view is helpful to understand the self-assembling process of the 2D nanoclusters on a surface; when the nanocluster concentration increases to a critical value, the self-assembly starts to proceed due to the overlap of the "molecular orbit" of the 2D nanoclusters. Details about this issue will be discussed in the last subsection after the analysis of the $\sqrt{21}$-Au atomic structure in the next subsection.

B. Atomic structures of the Au nanocluster and $\sqrt{21}$-Au superstructure

Because of their similar electronic structure and STM images, the $\sqrt{21}$-Au and $\sqrt{21}$-Ag owever, even the most basic issue, that the number of Au or Ag adatoms in the $\sqrt{21}\times\sqrt{21}$ unit cell, has not been solved yet. The adsorption sites of the adatoms are also controversial. Based on their STM observations in early days, Ichimiya, *et al.* thought that three adatoms locate on Si trimers,[24] while Nogami, *et al.* believed five[25] and Tong *et al.* proposed four adatoms[26] sitting on the Ag triangles of the $\sqrt{3}$-Ag substrate. Later, Aizawa, *et al.* reported in their first-principles theory study that the adsorption on the Ag triangles is energetically more favorable than on the Si trimers.[42] In the surface X-ray diffraction experiment, Tajiri, *et al.* evidenced a typical interatomic vector existing in the Patterson map of the $\sqrt{21}$-Au structure, and with this result they proposed a new model with five adatoms sitting on the Ag triangles.[28]

Contrary to the previous STM studies that have only analyzed the $\sqrt{21}$-Au superstructure itself,[24,25] we start with the Au nanocluster, the basic building block of the $\sqrt{21}$-Au, because of its relative simplicity. Figures 4(a)–4(d) show a bias dependence of LT-STM images of a single Au nanocluster. Both of the empty- and filled-state STM images near Fermi level in Figs. 4(a) and 4(c), respectively, appear identical to those of "Ag propellers" reported previously for excess Ag adatoms on the $\sqrt{3}$-Ag substrate,[33] which confirms again the similarity of Au and Ag adsorptions on this substrate. Figure 4(d) displays a similar appearance with a stronger contrast to show clearly seven bright protrusions within the Au nanoclusters. When the tip bias is decreased to −1.80 eV, the Au nanocluster becomes cloudy with weak contrast inside, as shown in Fig. 4(b).

Since the substrate of $\sqrt{3}$-Ag is also clearly displayed around the Au nanocluster in the STM images, we can easily find the positions of the seven bright protrusions in the Au nanocluster with respect to the $\sqrt{3}$-Ag substrate. This is done by superimposing a hexagonal lattice net on the STM image as shown in Fig. 4(e), in which the vertexes are on the centers of Si trimers in the IET model of the $\sqrt{3}$-Ag surface as shown in Fig. 4(f). All of the seven bright protrusions in the Au nanocluster are found to locate on the Ag triangles of the $\sqrt{3}$-Ag substrate. This result is consistent with some previous STM observations,[25,26] but in contradiction with another one.[24] The STM images themselves taken by different researchers were basically the same, but with different levels of resolution. The inconsistency among the literature came

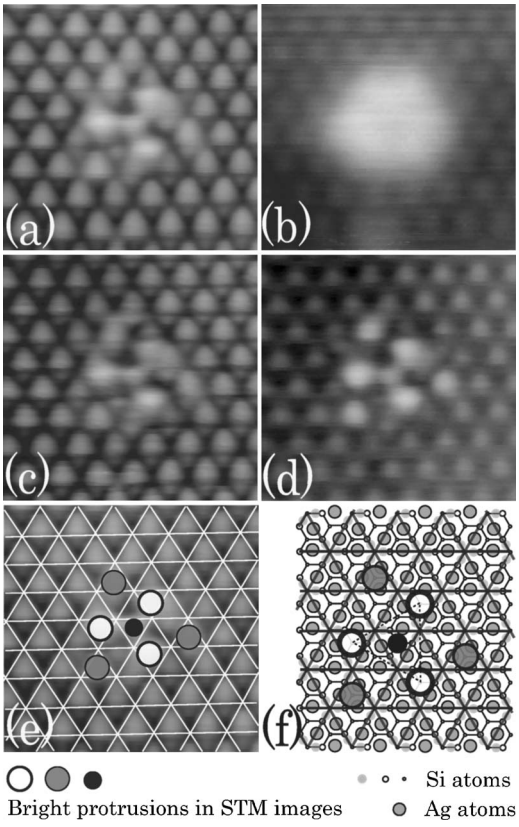

FIG. 4. Enlarged topographic LT-STM images of a single Au nanocluster taken at ~65 K at the same tunneling current of I =0.75 nA and various bias voltages: (a) V_{tip}=−0.20 V, (b) V_{tip}= −1.80 V, (c) V_{tip}=0.10 V, (d) V_{tip}=0.40 V. (e) The same STM image as (a), on which is superimposed a hexagonal lattice whose vertexes are at the center of Si trimers of the $\sqrt{3}$-Ag substrate. (f) IET model for the $\sqrt{3}$-Ag, on which several circles show the relative position of bright protrusions in the STM images of Au nanocluster.

from the assignment of the protrusion registry with respect to the $\sqrt{3}$-Ag substrate.

The seven protrusions in Fig. 4(f) are, furthermore, divided into three types according to their brightness: the first corresponds to the one at the center of cluster as indicated by a black circle, the second corresponds to the three strongest protrusions around the center as indicated by three open circles, and the third corresponds to the three gray circles at the corner of the cluster. As described later, some of the protrusions are Au adatoms, while the others are the results of electronic modulations.

Another important finding from the analysis of protrusions in the Au nanocluster is the threefold symmetry (though this is not surprising because the substrate of $\sqrt{3}$-Ag itself has such a symmetry). The possible number of Au adatoms in an Au nanocluster should be limited to 1, 3, 4, 6, 7,…, due to this threefold symmetry. It is worth noting that 5 Au adatoms cannot form such an Au nanocluster since they are impossible to be arranged in a threefold symmetry as long as none of them is piled up. Then, by combining the conclusion we made before that the Au nanocluster is the basic building unit of the $\sqrt{21}$-Au superstructure, we exclude any five-adatom structure models of $\sqrt{21}$-Au, in which five Au adatoms are assumed in the $\sqrt{21}\times\sqrt{21}$ unit cell.[25,28] Tong's model[26] is not correct either since it has no threefold symmetry.

Thus, none of the reported $\sqrt{21}$-Au atomic structure models is consistent with our STM images, and accordingly, a new structure model is required to be built. It is useful to determine first the number of Au adatoms in the $\sqrt{21}$-Au unit cell, which equals to the number of Au adatoms in the single Au nanocluster. As mentioned above, only 1, 3, 4, 6, 7,…, adatoms are possible by taking into account the threefold symmetry of the Au nanocluster. The number of 1 and those larger than 5 can be easily excluded experimentally within error by the evaporating rate of Au source calibrated by RHEED observation. We think that three-adatom is much more reasonable than four-adatom model mainly because of two PES experimental results. One is the change of surface-state bands near Fermi level (E_F) during the formation of the $\sqrt{21}$-Au superstructure. According to the previous ARPES results, the surface-state bands of the $\sqrt{3}$-Ag substrate shift toward higher binding energy due to electron transfer from Au adatoms to the $\sqrt{3}$-Ag substrate,[17,20] When the $\sqrt{21}$-Au superstructure is formed, Crain *et al.* counted the number of electrons in the unit cell from the Fermi circle using Luttinger's theorem, concluding about three electrons per $\sqrt{21}$-Au unit cell.[21] Because the substrate of $\sqrt{3}$-Ag has much smaller number of electrons in the surface-state band (about 0.02 electrons per $\sqrt{3}$ unit cell[32]), almost all of the three electrons in the surface state are thought to be transferred from the Au adatoms. By assuming that each Au adatom contributes one unpaired s,p electron, it is natural to think that there are three Au adatoms per $\sqrt{21}$-Au unit cell. Another PES experiment supporting this coverage is a quantitative analysis of the evolution of Si $2p$ core-level spectra. We found that after the formation of $\sqrt{21}$-Au superstructure, the first Si layer atoms can be classified into two groups according to their changes in binding energy of Si $2p$ CL due to Au adsorption. By assuming one Au adatom affects the chemical environment of three first-layer Si atoms nearby, we concluded that the model of three Au atoms in each $\sqrt{21}$-Au unit cell well explains the intensity ratio between the two groups of Si layers. On the contrary, any four- or five-adatom $\sqrt{21}$-Au model is not consistent with the results of Si $2p$ core-level experiments. The details are discussed in the next subsection.

Therefore, we can conclude that the saturation Au coverage for the $\sqrt{21}$-Au formation is 3/21=0.143 ML. Conversely, the Au coverage in the STM images in Fig. 3 was calibrated by counting the number of Au nanoclusters, each of which contains 3 Au atoms. In Fig. 3(a), for example, there are around 40 Au nanoclusters (means around 120 Au adatoms) in the image so that the Au coverage is estimated to be 0.016 ML. This calibration result agrees with that of rough calibration with RHEED observation mentioned in Sec. II.

The second step to build the atomic structure model of the $\sqrt{21}$-Au superstructure is to determine the Au adsorption site. Aizawa *et al.* have demonstrated in their first-principles calculations that the adsorption of adatoms on the center of Ag triangle is energetically more stable than on the Si trimer on the $\sqrt{3}$-Ag substrate.[42] This agrees well with the LT-STM

images in Fig. 4 that all the protrusions are located on the Ag triangle center, which indicates that some of them correspond to the Au adatoms, as expected in the previous STM studies of the $\sqrt{21}$-Au surface.[24–26]

As mentioned before, three types of protrusions in the Au nanocluster have been identified according to the brightness as shown by different circles in Figs. 4(e) and 4(f). By considering that adsorption of an Au adatom, in general, may induce some electronic modulation around it, it is natural to think that the inner protrusions indicated by three open circles correspond to the Au atoms. In the IET model of the $\sqrt{3}$-Ag surface, the two Ag triangles in the neighboring half unit cells are inequivalent in size and brightness in the STM images: the larger triangle is darker while the smaller one is brighter.[34] It is seen from Figs. 4(e) and 4(f) that the inner Au protrusions indicated by open circles are on the larger Ag triangles, while the outer ones indicated by gray circles are on the smaller Ag triangles. These two types of protrusions have slightly different bias dependence of the contrast: in Fig. 4(d), both of them appear very bright compared to the protrusions of the $\sqrt{3}$-Ag substrate; while in Figs. 4(a) and 4(c), the outer protrusions show weaker contrast than the feature of the $\sqrt{3}$-Ag substrate, leaving only three bright protrusions of the inner ones. It is reasonable to believe that the outer protrusions are essentially a result of some electronic modulation of the small Ag triangles in the $\sqrt{3}$-Ag substrate. Because of the influence of the Au adatoms nearby, these Ag triangles appear extra brighter at certain bias in STM images. Similarly, the center protrusion indicated by a black circle in the nanocluster is also considered as the result of a modulation in electronic states. Such a modulation is mainly due to the short-ranged interaction between the Au adatoms and the Ag triangles beneath, so it is not surprising that no obvious modulation in electronic states is seen outside the seven protrusions of an Au nanocluster. The speculations described above should be confirmed by theoretical simulations.

Another apparent evidence supporting these assignments of the protrusions is obtained in the aggregation of Au nanoclusters. Figure 5(a) is an enlarged LT-STM image of the $\sqrt{21}$-Au, which can be also viewed as an assembly of the Au nanoclusters. This STM image shows a much higher resolution than the previous ones performed at RT,[24,25] and appears similar to that of $\sqrt{21}$-Ag surface reported by Tong *et al.* at liquid N_2 temperature.[19] The features in this image can be explained well by the protrusions of the Au nanoclusters, one of which is indicated by the same set of circles as in Fig. 4(e). Figure 5(b) illustrates the aggregation of several Au nanoclusters whose protrusions are presented by the same set of circles. The protrusions in the $\sqrt{21}$-Au phase indicated by open circles keep the same separation with each other as in the Au nanocluster, so that they are connected by dot-lined triangles in order to clarify the Au nanoclusters. On the other hand, one outer protrusion indicated by a gray circle belongs to three surrounding nanoclusters. In other words, after aggregation, each gray-circle protrusion results from the contribution of three Au nanoclusters surrounding it. This is also the reason why they appear even brighter in Fig. 5(a) than the open-circle protrusions, each of which results from only one Au nanocluster. If the Au atoms in a cluster were located at the gray-circle sites, they would overlap with each other,

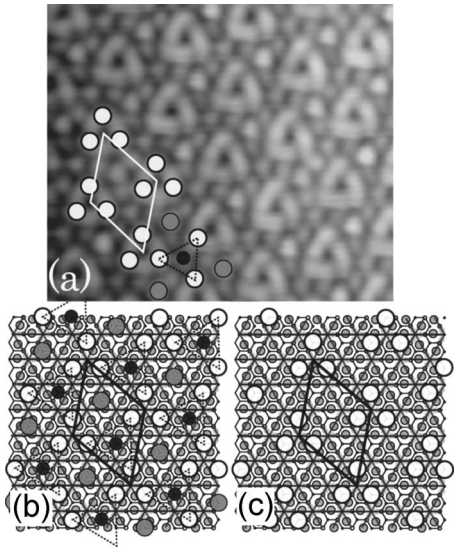

FIG. 5. (a) Enlarged topographic LT-STM image of the $\sqrt{21}$-Au superstructure at $V_{tip}=-1.00$ V and $I=0.60$ nA. One of the Au nanoclusters at the bottom of the image is indicated by a set of circles in agreement with Fig. 4(e). A $\sqrt{21}$-Au unit cell is also shown by a quadrilateral with open circles at the corners indicating the position of Au adatoms according to the new atomic structure model proposed in (c). (b) Diagram of bright protrusions on the $\sqrt{3}$-Ag substrate, illustrating the formation of $\sqrt{21}$-Au superstructures from the Au nanoclusters. (c) Our atomic structure model for the $\sqrt{21}$-Au superstructure proposed by considering that only the protrusions indicated by open circles in (b) correspond to Au adatoms.

making three Au atoms pile up at the grey-circle sites, or two-thirds of them would go away during the cluster aggregation, leaving only one Au atoms in each $\sqrt{21}$-Au unit cell. These are obviously not plausible. The most reasonable adsorption sites for Au adatoms therefore should be at the open-circle protrusions.

All the previous studies of the $\sqrt{21}$-Au surface have assumed that the framework of $\sqrt{3}$-Ag substrate is basically unaltered. This assumption is supported by the ARPES results showing that all the surface-state bands of $\sqrt{3}$-Ag substrate remain in the $\sqrt{21}$-Au (Ref. 20) and $\sqrt{21}$-Ag (Ref. 17) surfaces, while the bands only shift toward higher binding energy. With this assumption and based on the above conclusions that Au atoms sit on the open-circle protrusions, we propose an atomic structure model for the $\sqrt{21}$-Au superstructure shown in Fig. 5(c). Different than the previous models that used the honeycomb-chained triangles (HCT) structure for the $\sqrt{3}$-Ag substrate, the IET model is adopted here. In Fig. 5(c), the $\sqrt{21}$-Au unit cell is shown by a quadrilateral whose vortexes are set on the centers of Si trimers. Around each corner of the $\sqrt{21}$-Au unit cell, three Au atoms, which originally belong to three different Au nanoclusters, sit on the large Ag triangles of the IET half unit cell of the $\sqrt{3}$-Ag substrate. We believe this atomic model of $\sqrt{21}$-Au is also valid for the $\sqrt{21}$-Ag superstructure since they show so strong similarities in STM and PES results.

It is worth mentioning that during the submission of this report, Fukaya *et al.* reported their studies of the $\sqrt{21}$-Ag

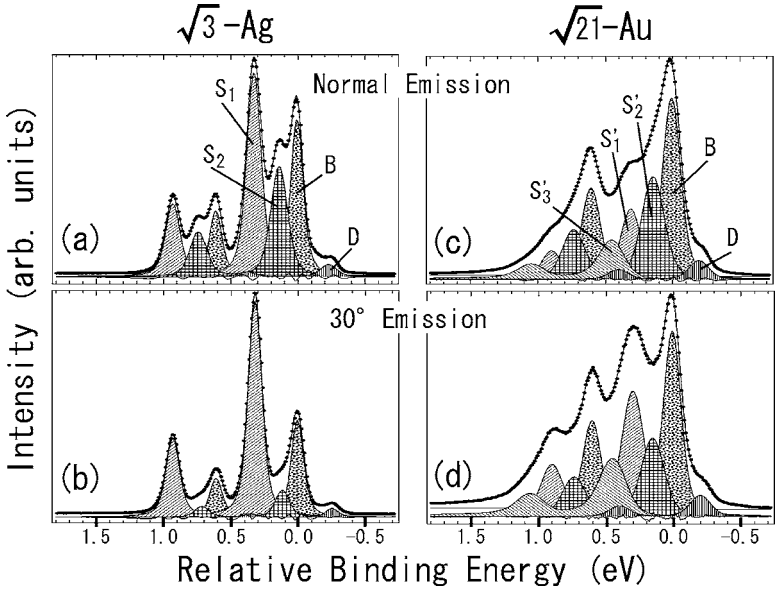

FIG. 6. Si 2*p* core-level spectra from the $\sqrt{3}$-Ag [(a), (b)] and $\sqrt{21}$-Au [(c), (d)], recorded at 70 K with photon energy of 135 eV at normal [(a), (c)] and 30° [(b), (d)] emissions. Parameters used in the fitting procedure to resolve the components are as follows: In the spectra of $\sqrt{3}$-Ag and $\sqrt{21}$-Au, the spin-orbit splittings are 0.605±0.003 and 0.595±0.005 eV, branching ratios 0.38±0.02 and 0.41±0.03, singularity 0 and 0.04, respectively. Lorentzian widths are fixed at 80 meV for all the spectra, while Gaussian widths are varied. For the $\sqrt{3}$-Ag, it is 65 meV for the bulk (B) and 95±10 meV for the surface (S_1 and S_2) components. For the $\sqrt{21}$-Au, it is 110 meV for bulk, 150±10 meV for S_1' and S_2', and 180 meV for S_3' components.

atomic structure with reflection high-energy positron diffraction.[29] The atomic structure model proposed in Fig. 5(c) agrees with their results.

C. Si 2*p* core-level photoemission spectroscopy

The CL-PES provides an effective method to study the chemical environment, local geometric structure and nature of chemical bonding centered around one atomic site, therefore it is a powerful tool to justify an atomic structure model or provide important structural information from another point of view. Here we investigated the Si 2*p* CL-PES of the $\sqrt{21}$-Au superstructure as well as the pristine $\sqrt{3}$-Ag surface, finding that there are three Au atoms in each $\sqrt{21}$-Au unit cell after a careful quantitative analysis.

The Si 2*p* CL-PES from the $\sqrt{3}$-Ag substrate have been investigated by many researchers for a dozen of years.[18,43,44] Recently Uhrberg *et al.* obtained a high-resolution spectrum of this surface, in which all surface-shifted components can be recognized directly and clearly from the raw spectrum.[43] In Fig. 6(a), we reproduced the high-resolution Si 2*p* core-level spectrum under a similar measurement condition with theirs.[43] Following their deconvolution[43], we decompose the spectrum with two surface (S_1 and S_2), one bulk (B) and one defect (D) components. The two surface components, S_1 and S_2, which shift from the bulk by 0.32 and 0.12 eV toward higher binding energy, are assigned to the atoms of the first (Si trimers) and second Si layer, respectively. The atoms in the third Si layer are in a bulklike environment and may not give rise to any significant energy shift in the spectra. We note that the Si 2*p* spectrum in Fig. 6(a) looks almost identical to those of Uhrberg *et al.*[43]

This deconvolution is confirmed by analyzing the Si 2*p* spectrum taken at an emission angle of 30° that has higher surface sensitivity, shown in Fig. 6(b). After a similar fitting procedure as for the normal-emission spectrum, the 30°-emission spectrum is also well resolved with the same set of components at corresponding relative binding energies. The remarkable change in the spectra from normal to 30° emissions is that the intensity of S_1 surface component increases relative to the bulk-component intensity, while that of S_2 significantly decreases. This is naturally explained in terms of electron escape depth, which reaches the maximum at the normal emission for any electron energy.

When the $\sqrt{21}$-Au superstructure is formed, the Si 2*p* spectra significantly change in shapes, as shown in Figs. 6(c) (normal emission) and 6(d) (30° emission). A similar fitting procedure for deconvolution has been also applied in order to obtain more detailed information. The spectra are resolved with three surface (S_1', S_2', and S_3'), one bulk (B) and one defect (D) components. Most of the parameters used here are similar to those for the $\sqrt{3}$-Ag surface, except for the singularity. Uhrberg *et al.* found that excess Ag atoms on the $\sqrt{3}$-Ag surface would bring an asymmetric tail on the higher binding energy side of the Si 2*p* core-level peak. In our experiment, during Ag deposition to prepare the $\sqrt{3}$-Ag surface, the Si wafer was kept at 450 °C, and an additional post-annealing of about two minutes at the same temperature was performed. Such a procedure left few excess Ag atoms on the surface so that the $\sqrt{3}$-Ag spectra shown in Figs. 6(a) and 6(b) do not exhibit such an asymmetric tail. Accordingly, the singularity was set to be 0 in the fitting procedure for the $\sqrt{3}$-Ag surface. On the other hand, for the $\sqrt{21}$-Au superstructure which is proved to be metallic by previous ARPES experiment,[19] a singularity index of 0.04 had to be introduced to reproduce the asymmetric tail.

According to the fitting results in Figs. 6(c) and 6(d), the three surface components S_1', S_2', and S_3' shift from the bulk component by 0.30, 0.14, and 0.44 eV, respectively, toward higher binding energy. Comparing to the energy shift of S_1 and S_2 in the $\sqrt{3}$-Ag surface, we believe that S_1' and S_2' have the same origins with S_1 and S_2, respectively. Namely, S_1' corresponds to the first layer Si atoms that have been affected very weakly by Au adatoms, while S_2' corresponds to the second layer Si atoms whose chemical surroundings are almost unchanged by the Au adatoms. This assignment is confirmed by their intensity changes between normal and 30° emissions. By comparing Figs. 6(c) with 6(d), we see that the

intensity of S_1' increases, while that of S_2' decreases. This is the same behavior as for S_1 and S_2 of $\sqrt{3}$-Ag in Figs. 6(a) and 6(b). We notice that S_1' of the $\sqrt{21}$-Au surface shows a fairly smaller intensity than S_1 of the $\sqrt{3}$-Ag surface, although they have the same origin of the first layer Si atoms. This indicates that there are some other Si atoms in the first layer that are quite influenced by the Au adatoms so that their Si $2p$ energy shift may be different from that of the S_1'. This is exactly the reason why the third surface component S_3' is needed in resolving the Si $2p$ core-level emission from the $\sqrt{21}$-Au. In other words, the S_3' corresponds to the first Si layer atoms whose chemical surrounding has been changed considerably by the Au adatoms. Such an assignment is consistent with the fact that the S_3' intensity increases as the S_1 and S_1' intensities do when the emission angle is increased to 30°.

The $\sqrt{3}$-Ag superstructure is formed by 1 ML Ag adsorption on the Si(111) crystal surface, which means each Ag atoms saturates one Si dangling bond. According to our atomic structure model for the $\sqrt{21}$-Au proposed in Fig. 5(c), one Au adatom locates at the center of an Ag triangle consisting of three Ag atoms in the $\sqrt{3}$-Ag substrate. This indicates that one Au adatom may have strong influence on the chemical environment of three Si atoms underneath through each Ag atom in the Ag triangle. That is to say, in each $\sqrt{21}$-Au unit cell, nine Si atoms may be strongly affected by the three Au adatoms, while the other 12 Si atoms in the first Si layer may not be affected so much. If it is the case, the intensity ratio between the S_3' and S_1' should be 9:12. From Figs. 6(c) and 6(d), we counted that the intensity ratio is 9.4:11.6 and 8.2:12.8, respectively. We have also done a similar analysis on the CL-PES spectrum of the same $\sqrt{21}$-Au sample surface taken at a larger emission angle (60°) and found a similar intensity ratio, 9.4:11.6, between S_3' and S_1' components (not shown here). Comparing the experimental results with the estimated ratio value, therefore, we concluded that this intensity analysis offers a strong evidence that supports our newly proposed structural model, in which each $\sqrt{21}$-Au unit cell has 3 Au adatoms. Simultaneously, it also clearly excludes the previously reported atomic models with 4 or 5 Au atoms in each $\sqrt{21}$-Au unit cell, because from these models it was expected that the intensity of S_3' should be larger than that of S_2', which conflicts with the experimental results.

It is worth noting that the shape of Si $2p$ CLS changed dramatically for various Au coverages less than 0.14 ML (the saturation coverage of Au for the $\sqrt{21}$-Au superstructure). The spectra with a deficit of Au (but showing a weaker $\sqrt{21}\times\sqrt{21}$ LEED pattern) were better described by superposition of the Si $2p$ core-level spectrum of the complete $\sqrt{21}$-Au surface and that of the surface covered only by the Au nanoclusters (without $\sqrt{21}\times\sqrt{21}$ LEED pattern).[45] Therefore, we must be very careful about the Au coverage; even if the LEED or RHEED shows a clear $\sqrt{21}\times\sqrt{21}$ pattern, the correct shape of Si $2p$ core-level spectra for the optimal $\sqrt{21}$-Au surface may not be obtained if the Au coverage is not saturated. There have been many investigations on the Si $2p$ CL-PES for various $\sqrt{21}\times\sqrt{21}$ surfaces including $\sqrt{21}$-Ag,[18,46] $\sqrt{21}$-Na,[46] and $\sqrt{21}$-K and $\sqrt{21}$-Cs.[22] Although they are formed by different metal atoms, we believe the same issue about the adatom coverage is important.

D. A condensation model: From surface molecules to surface superstructure

Finally, we discuss the stability and the self-assembly mechanism of the Au nanoclusters, proposing a condensation model for the $\sqrt{21}$-Au surface superstructure. ARPES experiments have revealed that each Au adatom transfers one electron to the substrate and turns to a cation.[19,21,47] As a result, the substrate is negatively charged and the Au cations are attracted by it. But such an electrostatic interaction as well as a possible van der Waals bonding between them is so weak that single Au adatoms keep migrating on the surface at RT. Its mobility is significantly reduced only when three Au adatoms aggregate into a nanocluster at LT.

An interesting question is how and why only the nanoclusters consisting of three adatoms can be stable in spite of the repulsive electrostatic interactions among the Au cations. With only the adatom-substrate bonding, it is not enough to explain that all the Au nanoclusters are identical, since there are still unoccupied adsorption sites around them. We noticed that the three Au adatoms form an equilateral triangle with a side of $3a_0$ [Fig. 4(f)], where a_0 is the length of the 1×1 Si(111) surface unit vector. The interatomic distance (11.52 Å) is so larger than an Au atomic radius (1.35 ~ 1.74 Å) (Ref. 48) that a direct covalent or ionic bonding among Au adatoms is not expected. Recent theoretical and experimental researches have revealed that indirect substrate-mediated interaction can be significant enough to influence the formation of nanostructures on surfaces.[11] The substrate-mediated interactions from neighboring adsorbates can combine constructively or destructively based on adsorbate separations. The DFT calculations[11] of Fichthorn *et al.*'s have revealed that on a metal surface, there are inevitable repulsive barriers for an adsorbate to join a nanostructure, which can be a monomer, dimer, trimer, and so on. The repulsion surrounding a monomer is very weak, while the barrier surrounding a dimer or a linear trimer is anisotropic so that there are relatively low-barrier paths for an adsorbate to approach them. However, the repulsion surrounding a compact trimer (in a triangle shape) is isotropic and the low-barrier paths no longer occur. Furthermore, it is pointed out that a linear trimer can easily rearrange to a more stable triangle form.[11] If these theoretical results obtained from the systems of metal adsorbates on metal surfaces are also applicable to the present Au/$\sqrt{3}$-Ag system, it is easy to understand the stability and the uniformity of the Au nanoclusters that consists of only three Au adatoms and forms a triangle shape. Such an assumption is reasonable since the dominant factor in this scenario is the electronic substrate-mediated interaction, and the $\sqrt{3}$-Ag surface is a typical 2D electron gas system that may be a good substrate to mediate such an indirect interaction.

Next, we discuss the self-assembly mechanism of the Au nanoclusters, proposing a condensation model for the $\sqrt{21}$-Au superstructure. It is seen from Fig. 5(b) that after self-assembly, three Au adatoms coming from three adjacent Au

nanoclusters form a smaller equilateral triangle with a side length of $\sqrt{3}a_0$. This Au-Au distance is much shorter than that within the Au nanocluster but still too long comparing to the Au atomic radius to form a direct covalent or ionic bonding among Au adatoms. van der Waals bonding may exist but should not be counted on to assemble them, since no such isolated small Au nanoclusters with the side of $\sqrt{3}a_0$ have been observed in STM. In fact, repulsive electrostatic interaction among these three Au adatoms should be strong to prevent them from aggregating in that way.

In Fig. 5(b), we notice that the self-assembly is actually the result that the corner Ag triangles (gray circles) of three adjacent Au nanoclusters overlap with each other. It is believed that this overlapping is the driving force for the self-assembly. To make this point clear and give a qualitative image, we regard the 2D Au nanoclusters as surface molecules that nucleate into a 2D crystal, i.e., the $\sqrt{21}$-Au superstructure. This analogy is reasonable because the Au nanoclusters behave as an unit in the self-assembly process. In this sense, the Au surface molecules include not only the three Au adatoms but also the surrounding Ag triangles of the $\sqrt{3}$-Ag substrate whose surface-state electrons are also modulated and stabilize the nanocluster electronically.

In this point of view, the corner Ag triangles (gray circles) can be viewed as a part of the 2D orientational "molecular orbits" corresponding to active sites for making bonds with the neighboring "molecules." When two or three of such surface molecules get close, their molecular orbits overlap, forming a bond between them, as illustrated in Fig. 7. The self-assembly proceeds as more surface molecules close up and join in. This model is an analogy to the formation of 2D supramolecular nanostructures from molecules such as fullerenes,[13] phthalocyanines[14] and napthalene tetracarboxylic di-imide (NTCDI) (Ref. 15) on the $\sqrt{3}$-Ag surface. These molecules diffuse freely on the surface, and form small domains in which the arrangement of molecules is predominantly governed by orientational intermolecular interactions.

It needs to be mentioned that the above discussion in this subsection is mainly a speculation based on the STM and CL-PES experimental results. To verify it, more studies including theoretical calculations are required.

IV. CONCLUSIONS

Identical Au nanoclusters have been found by LT-STM on the $\sqrt{3}$-Ag substrate, and the formation of $\sqrt{21}$-Au superstructure is revealed to be a self-assembly of the Au nanoclusters. At very low coverage (~0.02 ML), Au atoms tend to form the Au nanoclusters that are dispersed separately and randomly on the $\sqrt{3}$-Ag surface. As the coverage is increased, that is, the density of the Au nanoclusters is increased, the Au nanoclusters aggregate into the $\sqrt{21}$-Au superstructures. In other words, the Au nanoclusters are the building block of the $\sqrt{21}$-Au superstructure.

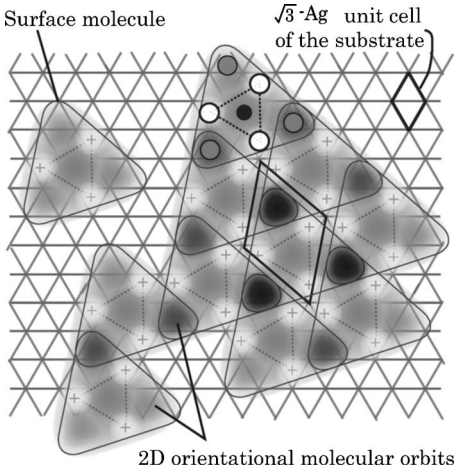

FIG. 7. Schematic illustration of the surface molecule and its organization into a small domain of $\sqrt{21}$-Au superstructure. The role of the Au nanocluster is indicated by a set of circles used in Figs. 4 and 5. A $\sqrt{21}$-Au unit cell is also indicated by a quadrilateral.

The stability and the uniformity of the Au nanoclusters are discussed in terms of substrate-mediated interactions between Au-Au adatoms. To conceptually explain the driving force of the self-assembling process, the Au nanoclusters are viewed as surface molecules with molecular orbits at the corners. When the surface molecules get close to each other, bonding due to overlap of the molecular orbits are formed, making the molecules regularly arranged.

With this point of view on the formation of $\sqrt{21}$-Au superstructure, we have revealed by careful LT-STM and CL-PES analysis that there are three Au adatoms within each Au nanocluster and each $\sqrt{21}$-Au unit cell. Additionally, all the Au adatoms are located on the Ag triangles of the $\sqrt{3}$-Ag substrate. Based on these conclusions, we proposed an atomic structure model for the $\sqrt{21}$-Au surface and excluded all previously proposed ones.

ACKNOWLEDGMENTS

T. Takahashi and H. Tajiri are sincerely appreciated for valuable discussions. M. D. thanks Bourse Lavoisier for financial support. This work has been supported by the Grants-In-Aid from the Japanese Society for the Promotion of Science.

*Electronic address: liu@surface.phys.s.u-tokyo.ac.jp

[1] P. L. McEuen, Science **278**, 1729 (1997).
[2] S. Sun, C. B. Murray, D. Weller, L. Folks, and A. Moser, Science **287**, 1989 (2000).
[3] L. Vitali, M. G. Ramsey, and F. P. Netzer, Phys. Rev. Lett. **83**, 316 (1999).
[4] J. Myslivecek, P. Sobotik, I. Ostadal, T. Jarolimek, and P. Smilauer, Phys. Rev. B **63**, 045403 (2001).
[5] M. Yoon, X. F. Lin, I. Chizhov, H. Mai, and R. F. Willis, Phys. Rev. B **64**, 085321 (2001).

[6] J.-L. Li, J.-F. Jia, X.-J. Liang, X. Liu, J.-Z. Wang, Q.-K. Xue, Z.-Q. Li, J. S. Tse, Z. Zhang, and S. B. Zhang, Phys. Rev. Lett. **88**, 066101 (2002).
[7] J.-F. Jia, X. Liu, J.-Z. Wang, J.-L. Li, X. S. Wang, Q.-K. Xue, Z.-Q. Li, Z. Zhang, and S. B. Zhang, Phys. Rev. B **66**, 165412 (2002).
[8] F. Silly *et al.*, Phys. Rev. Lett. **92**, 016101 (2004).
[9] P. Hyldgaard and M. Persson, J. Phys.: Condens. Matter **12**, L13 (2000).
[10] K. Lau and W. Kohn, Surf. Sci. **65**, 607 (1977); **75**, 69 (1978).
[11] K. A. Fichthorn and M. Scheffler, Phys. Rev. Lett. **84**, 5371 (2000); K. A. Fichthorn, M. L. Merrick, and M. Scheffler, Phys. Rev. B **68**, 041404(R) (2003).
[12] S. Hasegawa, X. Tong, S. Takeda, N. Sato, and T. Nagao, Prog. Surf. Sci. **60**, 89 (1999).
[13] M. D. Upward, P. Moriarty, and P. H. Beton, Phys. Rev. B **56**, R1704 (1997).
[14] M. D. Upward, P. H. Beton, and P. Moriarty, Surf. Sci. **441**, 21 (1999).
[15] D. L. Keeling *et al.*, Nano Lett. **3**, 9 (2003).
[16] X. Tong, C. S. Jiang, K. Horikoshi, and S. Hasegawa, Surf. Sci. **449**, 125 (2000).
[17] X. Tong, S. Ohuchi, N. Sato, T. Tanikawa, T. Nagao, I. Matsuda, Y. Aoyagi, and S. Hasegawa, Phys. Rev. B **64**, 205316 (2001).
[18] X. Tong, S. Ohuchi, T. Tanikawa, A. Harasawa, T. Okuda, Y. Aoyagi, T. Kinoshita, and S. Hasegawa, Appl. Surf. Sci. **190**, 121 (2002).
[19] X. Tong, C. S. Jiang, and S. Hasegawa, Phys. Rev. B **57**, 9015 (1998).
[20] H. M. Zhang, K. Sakamoto, and R. I. G. Uhrberg, Phys. Rev. B **64**, 245421 (2001).
[21] J. N. Crain, K. N. Altmann, C. Bromberger, and F. J. Himpsel, Phys. Rev. B **66**, 205302 (2002).
[22] H. M. Zhang, K. Sakamoto, and R. I. G. Uhrberg, Phys. Rev. B **70**, 245301 (2004).
[23] I. Matsuda, T. Hirahara, M. Konishi, C. Liu, H. Morikawa, M. D'angelo, S. Hasegawa, T. Okuda, and T. Kinoshita, Phys. Rev. B **71**, 235315 (2005); M. Konishi, I. Matsuda, C. Liu, H. Morikawa, and S. Hasegawa, e-J. Surf. Sci. Nanotechnol. **3**, 107 (2005).
[24] A. Ichimiya, H. Nomura, Y. Horio, T. Sato, T. Sueyoshi, and M. Iwatsuki, Surf. Rev. Lett. **1**, 1 (1994).
[25] J. Nogami, K. J. Wan, and X. F. Lin, Surf. Sci. **306**, 81 (1994).
[26] X. Tong, Y. Sugiura, T. Nagao, T. Takami, S. Takeda, S. Ino, and S. Hasegawa, Surf. Sci. **408**, 146 (1998).
[27] C. Liu, I. Matsuda, and S. Hasegawa, Surf. Interface Anal. **37**, 101 (2005).
[28] H. Tajiri, K. Sumitani, W. Yashiro, S. Nakatani, T. Takahashi, K. Akimoto, H. Sugiyama, X. Zhang, and H. Kawata, Surf. Sci. **493**, 214 (2001).
[29] Y. Fukaya, A. Kawasuso, and A. Ichimiya, Surf. Sci. **600**, 3141 (2006).
[30] R. Plass and L. D. Marks, Surf. Sci. **380**, 497 (1997).
[31] T. Nagao, S. Hasegawa, K. Tsuchie, S. Ino, C. Voges, G. Klos, H. Pfnur, and M. Henzler, Phys. Rev. B **57**, 10100 (1998).
[32] Y. Nakajima, G. Uchida, T. Nagao, and S. Hasegawa, Phys. Rev. B **54**, 14134 (1996).
[33] N. Sato, T. Nagao, and S. Hasegawa, Phys. Rev. B **60**, 16083 (1999).
[34] H. Aizawa, M. Tsukada, N. Sato, and S. Hasegawa, Surf. Sci. Lett. **429**, L509 (1999).
[35] N. Sato, T. Nagao, and S. Hasegawa, Surf. Sci. **442**, 65 (1999).
[36] I. Matsuda, H. Morikawa, C. Liu, S. Ohuchi, S. Hasegawa, T. Okuda, T. Kinoshita, C. Ottaviani, A. Cricenti, M. D'angelo, P. Soukiassian, and G. LeLay, Phys. Rev. B **68**, 085407 (2003).
[37] K. Kakitani, A. Yoshimori, H. Aizawa, and M. Tsukada, Surf. Sci. **493**, 200 (2001).
[38] Y. Nakamura, Y. Kondo, J. Nakamura, and S. Watanabe, Surf. Sci. **493**, 206 (2001).
[39] Y. Fukaya, A. Kawasuso, and A. Ichimiya, e-J. Surf. Sci. Nanotechnol. **3**, 228 (2005).
[40] H. Nakahara, T. Oya, Y. Saito, and A. Ichimiya, e-J. Surf. Sci. Nanotechnol.. **4**, 414 (2006), and references therein.
[41] J. A. Theobald, N. S. Oxtoby, M. A. Phillips, N. R. Champness, and P. H. Beton, Nature (London) **424**, 1029 (2003), and references therein.
[42] H. Aizawa and M. Tsukada, Phys. Rev. B **59**, 10923 (1999).
[43] R. I. G. Uhrberg, H. M. Zhang, T. Balasubramanian, E. Landemark, and H. W. Yeom, Phys. Rev. B **65**, 081305 (2002).
[44] S. Kono *et al.*, Phys. Rev. Lett. **58**, 1555 (1987); G. S. Herman *et al.*, Surf. Sci. **290**, L643 (1993); G. Le Lay *et al.*, Europhys. Lett. **45**, 65 (1998).
[45] C. Liu *et al.* (unpublished).
[46] M. D'angelo, M. Konishi, I. Matsuda, C. Liu, S. Hasegawa, T. Okuda, and T. Kinoshita, Surf. Sci. **590**, 162 (2005).
[47] C. Liu, I. Matsuda, R. Hobara, and S. Hasegawa, Phys. Rev. Lett. **96**, 036803 (2006).
[48] M. J. Winter, http://www.webelements.com/